DESIGN AND VALIDATION OF AN ENHANCED HOMOGENEOUS ISOTROPIC TURBULENCE CHAMBER

By

Ruiqi Wang

B.S.E., Case Western Reserve University, 2023

Thesis

Submitted in partial fulfillment of the requirements for the
Degree of Master of Science in the School of Engineering at Brown University

PROVIDENCE, RHODE ISLAND

MAY 2026

This thesis by Ruiqi Wang is accepted in its present form
by the School of Engineering as satisfying the thesis requirements
for the degree of Master of Science

Date________________ ____________________________

(Signature of Advisor)

Roberto Zenit, Advisor

Approved by the Graduate Council

Date________________ ____________________________

(Signature of Dean)

David P. Lindstrom, Dean of the Graduate School

AUTHORIZATION TO LEND AND REPRODUCE THE THESIS

As the sole author of this thesis, I authorize Brown University to lend it to other institutions or individuals for the purpose of scholarly research.

Date_________________ ______________________________

(Signature of Author)

Ruiqi Wang, Author

I further authorize Brown University to reproduce this thesis by photocopying or other means, in total or in part, at the request of other institutions or individuals for the purpose of scholarly research.

Date_________________ ______________________________

(Signature of Author)

Ruiqi Wang, Author

Preface and Acknowledgments

This thesis documents the design, construction, and initial validation of an enhanced homogeneous isotropic turbulence chamber developed in the School of Engineering at Brown University. The work builds directly on a previous laboratory chamber and focuses on the engineering redesign of the platform rather than on a complete turbulence-physics campaign. In particular, the present study centers on the enlargement of the chamber, the mechanical reconstruction of the system, the integration of encoder-based feedback, and the implementation of PID-assisted motor-speed synchronization.

The primary purpose of this thesis is to establish the redesigned chamber as a more capable experimental platform for future turbulence and multiphase-flow studies. Accordingly, the emphasis is placed on system development, control integration, and preliminary validation. While future work will require more extensive flow-field characterization, the contribution of the present thesis lies in creating and documenting the upgraded electro-mechanical platform that enables those later experiments.

This thesis is therefore intended both as a record of the chamber-development process and as a foundation for future investigations involving homogeneous isotropic turbulence, particle image velocimetry, and bubble-related experiments.

I would like to express my sincere gratitude to Professor Roberto Zenit for his guidance, support, and advice throughout this work. His direction and encouragement were essential to the development of this thesis.

I would also like to thank the members of the lab and the School of Engineering at Brown University for their help and support throughout my graduate studies. I am especially grateful to Madeline Federle, PJ Gaudio, and Anxu Huang; their insightful discussions, suggestions, and technical assistance contributed greatly to the success of this project.

In addition, I am grateful for the opportunity to work on this research topic and to develop my skills in experimental fluid mechanics, turbulence, and multiphase flow.

Finally, I would like to thank my family and friends for their patience, understanding, and encouragement throughout this process.

Table of Contents

List of Tables

List of Figures

Chapter 1

Introduction

1.1 Motivation

Turbulence remains one of the central problems in fluid mechanics because of its multiscale structure, strong fluctuations, and broad relevance to natural and engineering flows [1, 2]. Among turbulent configurations, homogeneous isotropic turbulence (HIT) is widely used as a canonical framework because its statistics are, ideally, uniform in space and independent of direction [1, 2]. Although perfect HIT cannot be achieved experimentally, laboratory devices can be designed to approximate it over a measurable region of the flow [3, 4].

Experimental HIT platforms are valuable because they provide controlled environments for turbulence measurements and for future studies involving dispersed phases such as bubbles [5, 4]. For this reason, the development of practical and controllable HIT chambers remains important in experimental fluid mechanics.

1.2 HIT as an Experimental Platform

The experimental generation of approximately HIT requires a balance between strong agitation and geometric symmetry [1, 3]. The forcing must generate sustained velocity fluctuations while limiting excessive mean circulation, and the chamber must also provide structural support, fluid containment, and optical access for diagnostics such as particle image velocimetry (PIV) [6, 7, 8].

Several approaches have been used to produce approximately HIT in the laboratory, including jet-stirred systems, enclosed fan-driven devices, and impeller-driven chambers [3, 9, 4]. Recent reviews have emphasized that non-grid methods remain an active area of development for the generation of zero-mean-flow homogeneous isotropic turbulence [10]. In the present work, the chamber is treated not only as a turbulence generator but also as a platform for future controlled experiments in turbulence and multiphase flow.

1.3 Prior Work and Need for Redesign

Previous work in the lab established an accessible, impeller-driven HIT chamber based on a truncated-cube geometry with eight impellers [4]. That device was experimentally characterized using PIV and was shown to generate flow with important features associated with approximately HIT, including near-isotropic velocity fluctuations in the central region, approximately Gaussian fluctuation distributions, and energy spectra consistent with Kolmogorov-type scaling [4].

That earlier chamber provided a strong baseline, but the next stage of development required two main improvements. First, a larger chamber was needed. Second, improved control of motor synchronization became desirable. The earlier study identified motor-speed variation as a possible source of departure from ideal forcing symmetry and suggested encoder-based feedback as a practical route for improvement [4]. These considerations directly motivated the redesign presented in this thesis.

1.4 Objectives and Scope of This Thesis

The objective of this thesis is to document the design, construction, and initial validation of an enhanced homogeneous isotropic turbulence chamber based on the previous laboratory platform. The work focuses on two main developments: enlargement of the chamber structure and integration of encoder-based, PID-assisted motor-speed control.

More specifically, this thesis presents:

- the mechanical redesign and construction of the enlarged chamber,
- the integration of encoders, updated control hardware, and PWM-distribution hardware,
- the implementation of a PID-based strategy for motor-speed balancing, and
- the initial system-level validation of the redesigned platform.

The scope of the thesis is centered on platform development rather than on a complete turbulence or bubble-breakup study. Future applications involving detailed flow characterization, PIV validation, and multiphase experiments motivate the chamber, but they are not the primary contribution of the present work.

The remainder of this thesis is organized as follows. Chapter 2 summarizes the relevant background and prior work. Chapter 3 defines the design requirements of the new chamber. Chapter 4 describes the mechanical design and construction. Chapter 5 presents the control architecture, encoder integration, and motor-speed balancing strategy. Chapter 6 discusses the initial validation and system characterization. Chapters 7 and 8 present the discussion, conclusions, and future work.

Chapter 2

Background and Literature Review

2.1 Fundamentals of HIT

Homogeneous isotropic turbulence (HIT) is one of the standard canonical configurations in turbulence research because it provides a simplified statistical framework for analyzing turbulent motion [1, 2]. In ideal HIT, the statistical properties of the turbulence are uniform in space and independent of direction. Although no laboratory system can produce perfectly homogeneous and isotropic turbulence, the HIT framework remains useful because it defines a clear basis for interpreting velocity fluctuations, characteristic scales, and spectral behavior [1].

In experimental studies of approximately HIT, the most relevant quantities are usually the mean velocity, the root-mean-square velocity fluctuations, the probability density functions of the fluctuations, and the turbulent energy spectrum [1, 2]. These metrics are commonly used to assess whether the flow is dominated by turbulent fluctuations rather than by strong mean circulation and whether the measured statistics are reasonably consistent with the expected behavior of approximately homogeneous isotropic turbulence.

2.2 Experimental Generation of HIT

The laboratory generation of approximately HIT requires distributed and approximately symmetric forcing while limiting large-scale directional flow structures [3, 9]. Several approaches have been used to produce approximately HIT in the laboratory, including jet-stirred systems, enclosed fan-driven devices, and impeller-driven chambers [3, 9, 4].

Recent reviews have highlighted that non-grid approaches remain an active area of development for zero-mean-flow homogeneous isotropic turbulence generation [10]. Additional laboratory platforms have also been reported for rapid turbulence generation and enclosed stirred configurations [11]. Some more recent facilities have been developed with explicit relevance to droplet and bubble fragmentation in strong turbulence [12, 13].

In addition to the forcing method, chamber geometry must also support structural integrity, fluid containment, and optical access for diagnostics such as particle image velocimetry (PIV) [6, 7, 8]. Detailed velocity-field measurements of approximately HIT in enclosed apparatus have also been demonstrated using PIV-based methods [14]. For compact laboratory systems, impeller-driven chambers are especially attractive because they can provide distributed forcing without requiring external recirculation loops and can often be fabricated and modified in-house [4].

This approach is particularly relevant to the present thesis, where the chamber is treated not only as a turbulence generator but also as a practical experimental platform for future turbulence and multiphase-flow studies.

2.3 Previous Chamber Developed in the Lab

The immediate foundation of the present work is a previous HIT chamber developed in the lab [4]. That device used a truncated-cube geometry with acrylic windows, a steel frame, and eight impellers located at the truncated corners. The chamber was designed as an accessible and relatively low-cost experimental platform that could be fabricated in-house while still supporting optical access and distributed forcing [4].

An important contribution of the earlier work was its experimental validation. PIV measurements showed that the chamber could generate flow with several important features associated with approximately HIT, including near-isotropic velocity fluctuations in the central region, approximately Gaussian fluctuation distributions, and energy spectra consistent with Kolmogorov-type scaling [4]. These results established the previous chamber as a viable baseline for further development.

2.4 Limitations of the Previous Design

Although the previous chamber was successful as a laboratory HIT platform, it also revealed limitations relevant to the next stage of development [4]. One important issue was variation in motor speed among the impellers. Because the chamber relies on distributed and approximately symmetric forcing, differences in motor speed can introduce forcing asymmetries and reduce the degree to which the generated flow approximates ideal HIT.

The earlier study suggested that encoder-based feedback control could reduce this limitation by improving motor-speed consistency [4]. In addition, the next stage of experiments required a larger chamber while preserving the useful features of the previous design, including distributed forcing, optical access, and practical manufacturability. These considerations motivated the redesigned chamber presented in this thesis.

Chapter 3

Design Requirements for the New Chamber

3.1 Motivation for the New Design

The redesigned chamber was motivated by the need to extend the previous laboratory HIT platform into a larger and more controllable experimental system [4]. The earlier chamber established the viability of the impeller-driven truncated-cube concept, but the next stage of development required both an increase in physical scale and improved control of motor synchronization. In particular, the previous study identified motor-speed variation as a possible source of forcing asymmetry and suggested encoder-based feedback as a practical route for improvement [4]. The present redesign therefore aims to preserve the useful features of the previous system while improving its scale, instrumentation, and controllability.

3.2 Functional Requirements

At the most basic level, the chamber must be able to generate a turbulent flow field that approximates homogeneous isotropic turbulence over a measurable region of the fluid volume [1, 4]. Although perfect HIT is not achievable in a real apparatus, the chamber should provide sufficiently symmetric forcing and sufficiently small mean flow to support future turbulence characterization and experimental use.

A second functional requirement is repeatable operation. The chamber should be capable of stable and repeatable runs so that future measurements can be compared under nominally similar forcing conditions. This is especially important for later PIV-based validation and for future multiphase-flow experiments involving bubbles or other dispersed phases [6, 5].

A third requirement is experimental accessibility. The chamber must provide optical access, practical access to the interior, and sufficient integration space for supporting hardware such as power distribution, control, and cooling subsystems. In this sense, the device must function not only as a turbulence generator but also as a practical laboratory platform.

3.3 Mechanical Requirements

Because the redesigned chamber is larger than the previous system, the mechanical design must provide sufficient rigidity, alignment, and sealing quality for reliable operation. The frame must support the chamber body and the distributed drive units without excessive deformation or misalignment, while the shaft interfaces must allow rotation through the chamber wall with minimal leakage.

Fluid sealing is a particularly important requirement because the chamber is intended for liquid-phase experiments. The enlarged body, removable top and bottom covers, and rotating shaft penetrations all introduce potential leakage paths, so the chamber must be designed with practical and robust sealing interfaces. Reliable shaft sealing is an important design requirement in rotating liquid-phase systems and becomes especially important at the chamber-wall penetration points used in the present apparatus [15, 16].

The mechanical design must also remain manufacturable and serviceable. Since one of the strengths of the previous chamber was its in-house fabrication philosophy [4], the redesigned chamber should preserve this practical character while accommodating a larger scale and a more complex corner-drive assembly.

3.4 Control and Instrumentation Requirements

The most important control requirement of the redesigned chamber is improved motor-speed synchronization. Because the chamber depends on distributed impeller forcing, differences in motor speed can reduce the symmetry of the forcing and affect the resulting flow field [4]. The new system therefore requires direct rotational-speed measurement for each motor and a control strategy capable of reducing motor-to-motor mismatch during operation.

This requirement motivates the integration of encoders and closed-loop control. The chamber must be able to measure motor behavior in real time, estimate RPM, and adjust motor commands accordingly. In the present work, this objective is addressed through encoder-based feedback, PWM distribution through external hardware, and PID-based motor-speed balancing.

The control architecture must also remain practical for a multi-motor laboratory system. It should support repeated operation, traceable operating conditions, and future refinement, while remaining compatible with the broader experimental role of the chamber as a platform for later flow characterization.

3.5 Summary of Design Goals

The design goals of the redesigned chamber can be summarized as follows: to create a larger HIT platform, to preserve the useful impeller-driven concept of the previous chamber, to improve motor-speed controllability through encoder-based feedback and PID-assisted balancing, and to maintain practical manufacturability and experimental accessibility. These goals define the engineering direction of the redesign and motivate the mechanical and control developments described in the following chapters.

Chapter 4

Mechanical Design and Construction

4.1 Overview of the New Chamber

The redesigned chamber was developed as an enlarged and improved version of the previous impeller-driven HIT platform [4]. Its purpose is to preserve the useful features of the earlier chamber while providing a larger structure and improved support for sensing, control, and future experiments. The new device remains based on distributed impeller forcing around a geometrically symmetric chamber, but its mechanical design was revised to accommodate a larger chamber body, updated corner drive units, and auxiliary subsystems.

Figure 1 shows the completed chamber as an integrated mechanical platform.

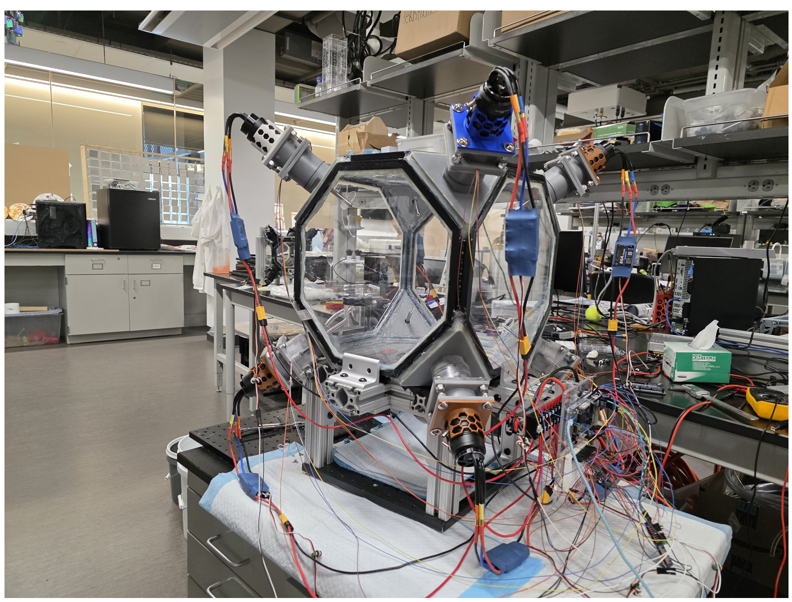

Figure 1: Overall view of the redesigned homogeneous isotropic turbulence chamber with eight corner-mounted drive units.

4.2 Chamber Geometry and Scaling

The redesigned chamber retains the general truncated-cube concept of the previous chamber, but at a larger scale and with revised corner interfaces [4]. The chamber body is formed by octagonal acrylic faces mounted within a welded steel-angle frame. Four panels are standard solid octagonal faces, while the remaining two are access panels: one bottom panel with a centered 4 in circular opening and one top panel with a centered 6 in circular opening. These openings are fitted with removable circular covers to improve draining, filling, and interior access.

The principal geometric scale of the chamber can be described by the spacing between opposing corner-mounted motors. This spacing is approximately 20 in, corresponding approximately to a cubic envelope of 20 in $\times$ 20 in $\times$ 20 in for the overall chamber scale. The octagonal edge length is approximately 5.5 in. These dimensions distinguish the redesigned chamber from the previous, smaller version and reflect the need for a larger experimental platform.

The principal dimensions of the chamber and the corner drive-unit components are summarized in Tables 1 and 2.

Table 1: Main dimensions of the redesigned chamber.

Component / Dimension	Value
Distance between two opposing corner motors	20 in
Approximate overall cubic envelope	20 in $\times$ 20 in $\times$ 20 in
Octagonal edge length	5.5 in
Bottom access opening diameter	4 in
Top access opening diameter	6 in

Table 2: Main dimensions of the corner drive-unit components.

Component / Dimension	Value
Total length of assembled corner motor unit (including shaft)	8 in
Triangular support piece height	1.5 in
Triangular support piece side length	5.5 in
Upper bottom support part height	1.875 in
Upper bottom support part square side length	3 in
Encoder support piece height	1.25 in
Encoder support piece square side length	3 in
Motor housing square base side length	3 in
Motor housing height	1.75 in
Circular motor-support region width	2 in

4.3 Structural Design

The chamber body consists of a welded steel-angle frame combined with acrylic panels inserted from the inner side of the chamber. The steel-angle ligaments were welded into octagonal faces and then assembled into the complete truncated-cube structure. This frame provides both the overall geometry of the chamber and the support lips needed to hold the acrylic faces. Triangular openings were intentionally left at the truncated corners so that the corner drive assemblies could be mounted there.

The acrylic panel set includes four standard face panels, one bottom access panel, and one top access panel. The bottom panel includes a 4 in opening and the top panel includes a 6 in opening, each with a matching circular cover. Rubber gaskets were placed between the covers and the corresponding acrylic panels. After installation, epoxy was applied to the structural interfaces and a silicone layer was added to improve sealing and reduce leakage. Reliable shaft and panel sealing is an important requirement in rotating liquid-phase systems and becomes especially significant at the chamber-wall penetration points used in the present apparatus [15, 16].

The chamber is mounted on an aluminum support platform that elevates the body above the base surface, improves access to the lower drive locations, and provides space for supporting hardware such as wiring, power distribution, and cooling components.

The welded steel-angle frame is shown in Figure 2, the acrylic panel set is shown in Figure 3, and a top view of the assembled chamber body is shown in Figure 4.

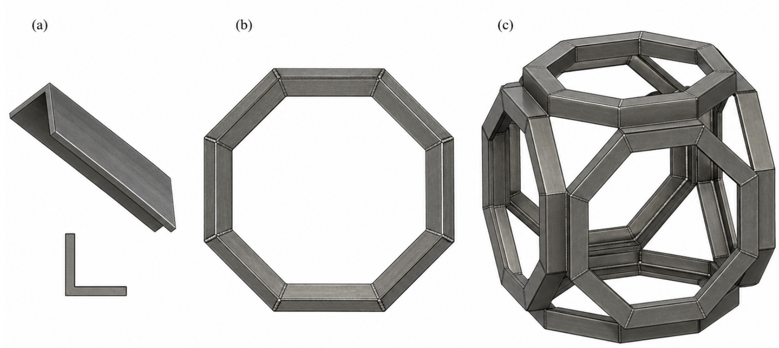

Figure 2: Steel-angle frame used for the redesigned chamber: (a) individual frame ligament with L-shaped cross section, (b) one assembled octagonal face, and (c) the complete welded chamber frame.

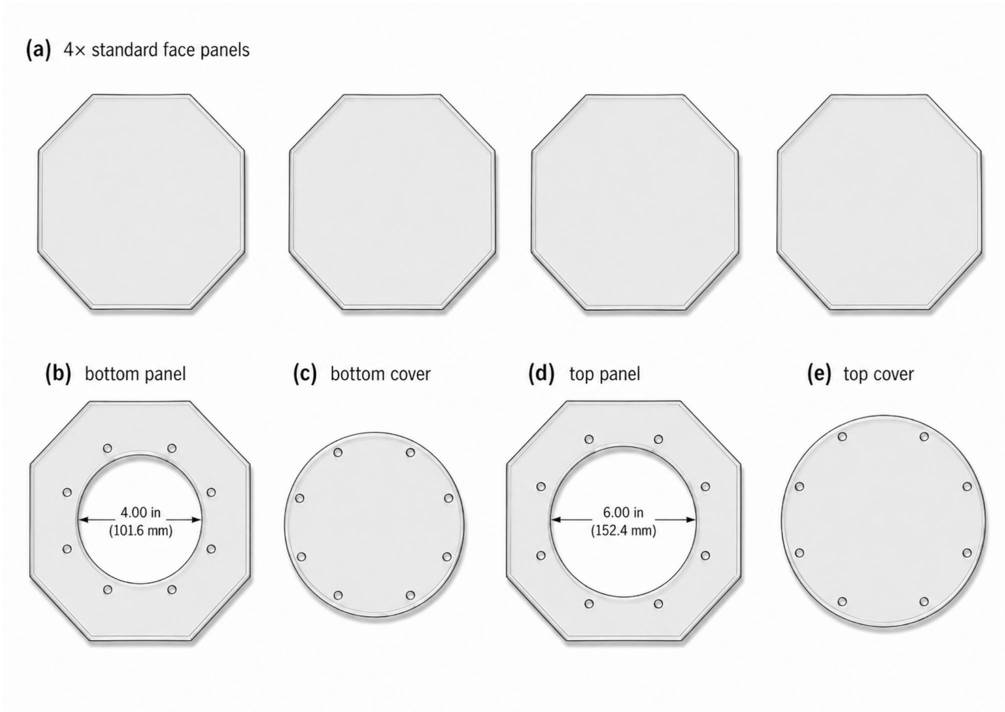

Figure 3: Acrylic panel set used for the redesigned chamber, including (a) four standard face panels, (b) the bottom panel with a 4 in circular opening, (c) the bottom cover, (d) the top panel with a 6 in circular opening, and (e) the top cover.

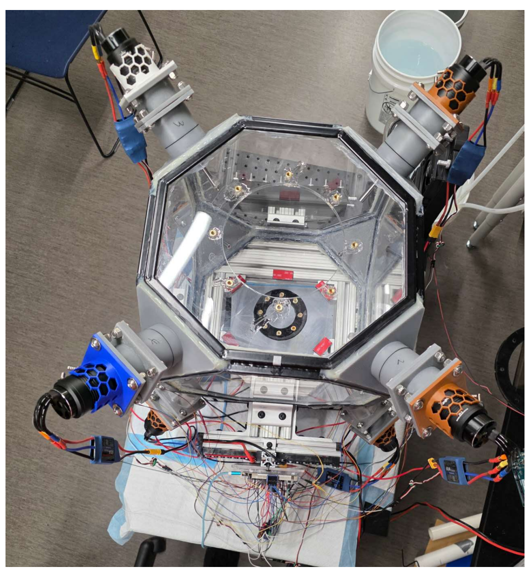

Figure 4: Top view of the assembled chamber body showing the inner acrylic faces, sealing regions, and access geometry.

4.4 Motor and Impeller Assembly

Each truncated corner of the chamber contains a dedicated drive assembly that transfers motor torque into the chamber through a sealed shaft interface. The chamber-side assembly begins with a triangular support piece mounted into the corner opening of the steel frame. A mechanical seal is inserted into the central opening of this support piece, and a rubber gasket is placed on the cylindrical sealing interface. The upper bottom support part is then aligned and fastened to complete the chamber-side support structure.

The motor-side assembly is built separately. A brushless motor is mounted inside a 3D-printed motor housing, after which the motor shaft is connected to an intermediate shaft using a 5-to-5 mm coupler. An encoder support piece is then added so that the encoder can be mounted in alignment with the shaft. A second coupling stage connects the intermediate shaft to the impeller-side shaft through a 5-to-8 mm coupler. The final 8 mm shaft extends through the chamber-side interface and supports the impeller inside the chamber.

The total assembled drive unit, including shaft, is approximately 8 in long. After insertion into the chamber-side support structure, the components are fastened together and a three-blade 3D-printed impeller is mounted on the exposed shaft end. This same assembly procedure is repeated at all eight corners.

A representative installed corner-mounted drive unit is shown in Figure 5, and the final impeller mounted inside the chamber is shown in Figure 6.

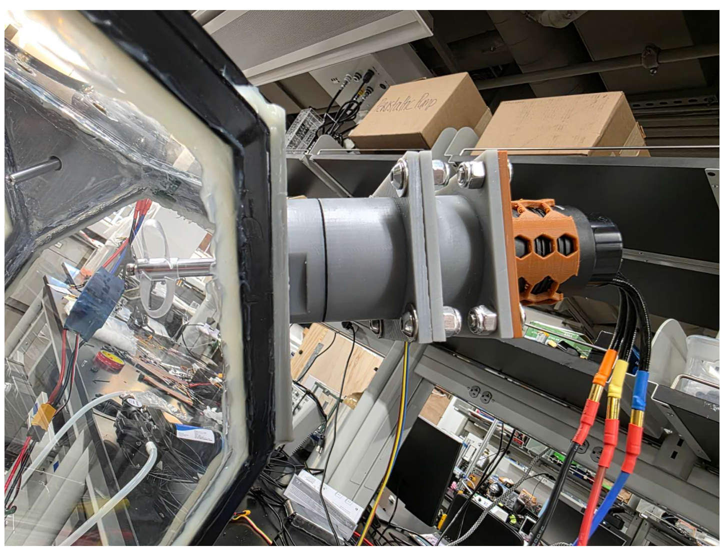

Figure 5: Representative installed corner-mounted drive unit after fastening to the chamber support structure.

Figure 6: Three-blade impeller mounted on the exposed shaft inside the chamber.

4.5 Fabrication and Assembly

The fabrication of the chamber followed a staged assembly process. The steel-angle ligaments were first welded into octagonal faces and then into the complete chamber frame. The acrylic panels were cut and inserted from the inside of the frame, with the top and bottom access panels aligned to accept the circular covers. Rubber gaskets were installed at the access interfaces, and epoxy followed by silicone was applied along the panel-frame boundaries to improve bonding and sealing.

Once the chamber body had been completed, the chamber-side corner supports were mounted into the triangular frame openings and sealed. The motor-side assemblies were then prepared separately by integrating the motor, housing, encoder piece, encoder, couplers, and shafts. Each completed drive module was inserted into the chamber-mounted support structure and fastened in place. The final step at each location was the installation of the three-blade impeller.

Because the chamber contains eight identical drive locations, the same procedure was repeated eight times. This repeated assembly process was important not only for completion of the chamber but also for maintaining consistency across the full impeller array.

4.6 Final Constructed System

The final constructed system integrates the enlarged chamber body, the welded frame, the acrylic faces, the eight corner-mounted drive units, and the interfaces needed for later control and instrumentation. At this stage, the chamber can be understood as a completed electro-mechanical platform that supports the next phase of the work, including encoder integration, motor-speed synchronization, and initial system validation.

Relative to the earlier device, the redesigned chamber incorporates a larger geometry, more complex corner drive assemblies, improved access covers, revised sealing, and provisions for additional hardware such as power distribution and water cooling. The result is not simply a larger copy of the previous system, but a more capable experimental platform [4].

The estimated cost of the redesigned chamber is grouped by major subsystem category in Table 3.

Table 3: Estimated cost breakdown of the redesigned chamber.

Category	Estimated cost (USD)
Water-cooling system	388.29
Electronic and signal hardware	549.00
Motor-drive components	683.00
Assembly and sealing components	641.00
Overall frame and chamber body	360.00
Total estimated cost	2621.29

Chapter 5

Control System and Encoder Integration

5.1 Control Architecture

The upgraded control architecture is built around an Arduino GIGA R1, which replaces the earlier Arduino Mega-based implementation. One important consequence of this change is the logic-voltage difference between the two controllers. Whereas the earlier Arduino Mega configuration operated at 5 V logic, the Arduino GIGA operates at 3.3 V logic. This required corresponding changes in the signal-conditioning and encoder-interface hardware. The redesign therefore extends the earlier chamber architecture while addressing its limited motor-speed observability [4].

In the present system, the Arduino GIGA serves as the main control and feedback-processing unit. It communicates with the host computer through USB and receives encoder signals from the eight corner drive units. These encoder measurements are used for RPM estimation and feedback-based motor balancing. The ESC control signals are not generated directly from the Arduino GIGA pins. Instead, a PCA9685 PWM driver module is used to distribute PWM commands to the ESCs. The Arduino GIGA communicates with the PCA9685 through the I^2C interface, with SDA connected to pin 20 and SCL connected to pin 21. This arrangement allows PWM generation to be handled externally, leaving the GIGA available for encoder reading and closed-loop computation.

The overall control structure therefore consists of three linked functions: command input from the laptop computer, PWM distribution from the PCA9685 to the ESC array, and encoder-based feedback processing by the Arduino GIGA. This architecture is particularly useful because the chamber contains eight motors and eight encoders, making direct simultaneous handling of all signal-generation and signal-analysis tasks by a single controller less practical. The overall control and power architecture of the redesigned chamber is shown in Figure 7.

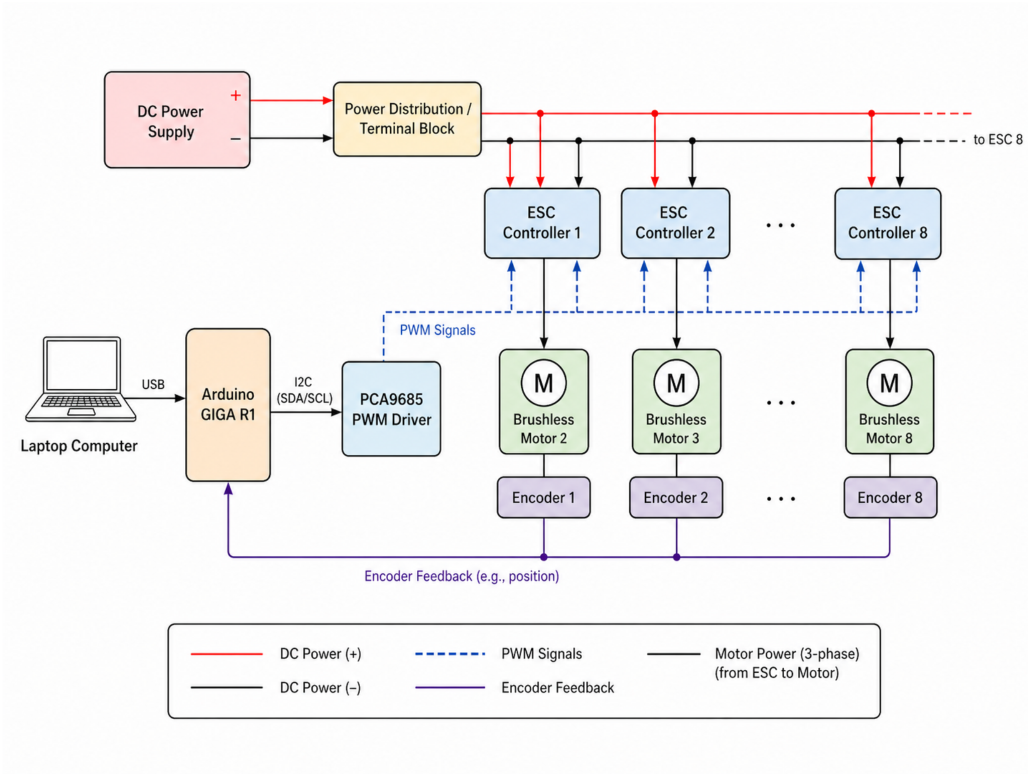

Figure 7: Schematic of the control and power architecture of the redesigned chamber, including the laptop computer, Arduino GIGA R1, PCA9685 PWM driver, ESC array, brushless motors, encoder feedback, terminal-based power distribution, and DC power supply.

5.2 Encoder Integration and Signal Wiring

Encoder integration is a central feature of the redesigned chamber because it provides direct rotational-speed feedback for each of the eight motors. One encoder is mounted to each corner drive unit, allowing the controller to estimate RPM during operation and compare the measured motor speeds across the full array.

The transition from the Arduino Mega to the Arduino GIGA made the encoder interface more demanding because the GIGA operates at 3.3 V logic rather than 5 V logic. To ensure signal compatibility, four level-shifting modules were introduced between the encoder hardware and the controller-side input stage. The encoder and ESC signal harnesses were organized by color to simplify wiring, assembly, and debugging. In the present system, brown wires correspond to encoder ground, yellow wires to encoder phase A, blue wires to encoder phase B, and orange wires to encoder supply. For the ESC-side signal wiring, white wires were used for the PWM control signal and black wires were used for ESC ground. Encoder and ESC grounds were tied together to maintain a common electrical reference.

The implemented controller-side hardware is shown in Figure 8, and the PCA9685 signal-distribution module is shown in Figure 9.

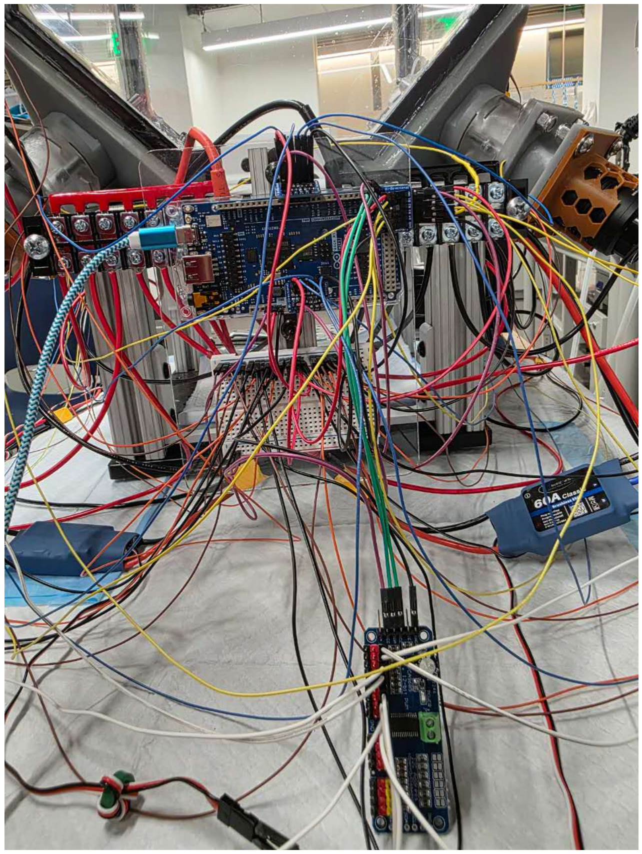

Figure 8: Arduino GIGA-based control hardware showing the controller, breadboard-level signal organization, and supporting encoder-interface wiring.

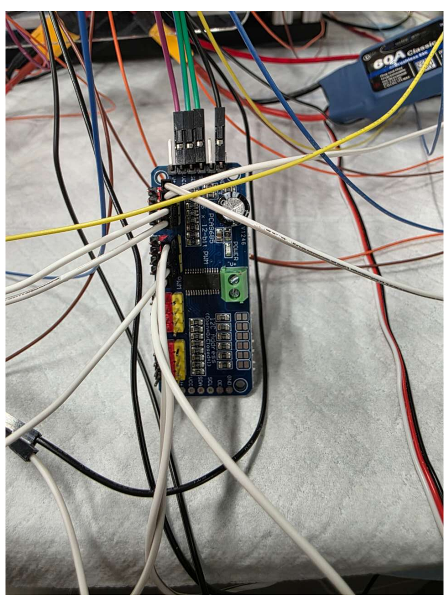

Figure 9: PCA9685 module used to distribute PWM control signals to the ESC array.

5.3 RPM Measurement

The integration of encoders makes it possible to estimate motor rotational speed in real time. In the present chamber, each motor is equipped with a US Digital E4T miniature optical encoder configured at 100 CPR (cycles per revolution). The encoder provides the incremental count data required for speed estimation, which is consistent with general sensor-based approaches to rotational measurement [17].

For motor i, let $N_i(t)$ denote the cumulative encoder count at time t. The count increment over one update interval is

$$\Delta N_i = N_i(t) - N_i(t - \Delta t), \tag{5.1}$$

where Δt is the elapsed time between successive control updates. In the present code, the control interval is approximately 20 ms. The elapsed time is computed from the Arduino millisecond timer according to

$$\Delta t = \frac{t_{\text{current}} - t_{\text{previous}}}{1000}, \tag{5.2}$$

so that Δt is expressed in seconds.

Using the encoder resolution $N_{\text{CPR}} = 100$, the motor speed is calculated as

$$\text{RPM}_i = \frac{|\Delta N_i|\,60}{N_{\text{CPR}}\,\Delta t}, \tag{5.3}$$

where the absolute value is used because the present control objective is speed balancing rather than directional control. In the code, the most recent encoder count is stored after each update and used as the reference for the next interval. The measured RPM values are printed to the serial monitor for real-time observation and are also used as feedback inputs to the controller.

After startup, once the motors have reached a usable operating condition, the controller computes the average speed of the full array and uses it as the common balancing target:

$$\text{RPM}_{\text{target}} = \frac{1}{8}\sum_{i=1}^{8} \text{RPM}_i. \tag{5.4}$$

In the current implementation, this target is accepted only if all motors have reached a minimum operating threshold; otherwise, the code delays target locking until a valid operating condition is obtained.

Direct RPM measurement is therefore important not only for monitoring single motors but also for evaluating mismatch across the full eight-motor system. If one or more motors operate at noticeably different speeds, the forcing applied to the chamber becomes less symmetric. RPM measurement thus provides both a diagnostic tool and the measurement layer required for closed-loop synchronization.

5.4 PID-Based Motor-Speed Balancing

Once RPM can be measured, the next requirement is a control strategy capable of reducing the difference between the measured and desired motor speed. In the redesigned chamber, this is addressed using PID-based control. PID control remains one of the most practical and widely used approaches for BLDC speed regulation and multi-motor synchronization problems [18]. Each motor has its own control error, integral history, and previous error value, so although all motors are intended to operate around a common target RPM, the PWM command sent to each ESC is adjusted individually according to the measured behavior of that motor.

For motor i, the control error is defined as

$$e_i(t) = \mathrm{RPM}_{\mathrm{target}} - \mathrm{RPM}_i(t), \tag{5.5}$$

where $\mathrm{RPM}_i(t)$ is the measured speed of motor i and $\mathrm{RPM}_{\mathrm{target}}$ is the common target speed for the array. The corrected PWM command is then computed in the form

$$\mathrm{PWM}_i = \mathrm{PWM}_{\mathrm{base}} + K_p e_i + K_i \int e_i \, dt + K_d \frac{de_i}{dt}, \tag{5.6}$$

where $\mathrm{PWM}_{\mathrm{base}}$ is the user-defined baseline PWM command and K_p, K_i, and K_d are the proportional, integral, and derivative gains. In the current implementation, the selected gains are

$$K_p = 0.026, \qquad K_i = 0.06, \qquad K_d = 0.00065. \tag{5.7}$$

To improve stability, the integral term is constrained within a fixed range before being used in the control update, and the final PWM command is also bounded within a safe operating range for the ESCs. The PID loop is executed at regular intervals of approximately 20 ms. At each update, the controller computes the current RPM of each motor, evaluates the error relative to the target speed, updates the integral and derivative terms, and sends the corrected PWM command to the corresponding ESC channel.

This closed-loop strategy is especially important in the present chamber because the eight-motor array is not uniform: four motors are rated at 3250 KV and four are rated at 2660 KV. Under these conditions, identical open-loop PWM commands do not imply identical operating speeds. Encoder-based PID correction is therefore required to reduce motor-to-motor mismatch and maintain a more symmetric forcing condition within the chamber. Related synchronization methods based on deviation coupling and improved cross-motor coordination have also been reported for multi-motor systems [19, 20]. The need for improved motor-speed consistency was already identified as a practical limitation of the previous chamber design [4].

5.5 Implementation

The upgraded control system combines encoder reading, RPM estimation, PWM distribution, and closed-loop motor-speed correction. The Arduino GIGA performs the feedback-processing tasks, while the PCA9685 handles PWM generation for the ESC array. This arrangement reduces the signal-handling burden on the main controller and makes the multi-motor system more practical to operate.

In the implemented wiring layout, encoder signals are routed through the level-shifting stage before entering the GIGA. Power for the encoder-side circuitry is distributed through the breadboard, and common grounding is maintained across the encoders, ESCs, logic converters, and controller. On the power side, ESC supply lines are routed through a terminal-based distribution board connected to the main DC power supply.

At the software level, the control loop repeatedly performs the following operations: initialize hardware, read user commands, acquire encoder counts, compute RPM, determine or update the target RPM, evaluate the PID error for each motor, update the PWM commands through the PCA9685, and display RPM and PWM values for monitoring. The resulting implementation follows the general structure of practical embedded closed-loop motor control systems, but is specialized here for an eight-motor turbulence chamber.

5.6 Initial Control Performance

The initial control performance of the upgraded system is evaluated in terms of its ability to support measurable and coordinated motor operation. Relative to the previous open-loop configuration, the redesigned chamber now provides direct RPM measurement, external PWM distribution, and encoder-based correction of motor-speed mismatch [4].

At the systems level, improved control performance is reflected in three practical indicators: the ability of the motors to reach a common operating range, the reduction of motor-to-motor mismatch during steady operation, and the ability of the full eight-motor system to operate in a measurable and repeatable way. The use of the PCA9685 for PWM distribution and the Arduino GIGA for feedback processing also improves task separation within the control system.

Although full turbulence validation depends on later flow diagnostics, the control developments reported here are already important because they establish the instrumentation and balancing capability required for future chamber characterization. In this sense, the present chapter provides the control foundation of the redesigned chamber, while the next chapter addresses its initial validation and system-level characterization.

Chapter 6

Initial Validation and System Characterization

6.1 Validation Objectives

The purpose of validation in the present work is to assess whether the redesigned chamber operates as an improved experimental platform and whether its current level of development supports future turbulence characterization. In the context of this thesis, validation is not limited to the final quality of the generated turbulence field. It also includes the practical readiness of the chamber as a physical system, including stable operation, consistent motor performance, and compatibility with future diagnostic measurements.

This broader interpretation is appropriate because the redesigned chamber represents a platform-development effort rather than a complete turbulence-physics campaign. Accordingly, the validation objectives of the present work can be summarized in three levels: system-level functionality, control-level performance, and flow-level readiness. The first concerns chamber integrity, assembly stability, and coordinated operation of the drive system. The second concerns encoder-based RPM measurement and motor-speed balancing. The third concerns the degree to which the chamber is prepared for future flow characterization using methods consistent with the previous chamber study [4].

6.2 Experimental Setup

The experimental platform used for initial system characterization includes the chamber itself, eight externally mounted brushless motors, eight ESCs, eight encoders, an Arduino GIGA controller, a PCA9685 PWM-distribution module, a breadboard-level signal-conditioning interface, a terminal-based power-distribution board, a switching DC power supply, and a water-cooling subsystem.

The main power source for the motor-drive system is a switching DC power supply connected to the ESC array through the terminal-based distribution board. This arrangement provides a centralized and repeatable way to distribute power to the eight ESCs while keeping the motor-drive current path separate from the controller-side signal wiring.

In addition to the electrical drive hardware, the setup includes a water-cooling loop for the motors. This subsystem was added because motor heating becomes a practical concern during prolonged multi-motor operation. The cooling system therefore improves the operational stability of the platform and reduces the likelihood that temperature rise will affect the repeatability of the drive behavior during testing.

The complete setup should therefore be understood as a platform-level experimental system rather than as a chamber body alone. Structural, mechanical, electrical, and control subsystems are all required for the chamber to operate as intended.

Figure 10: Switching DC power supply used to provide electrical power to the ESC array through the terminal-based distribution system.

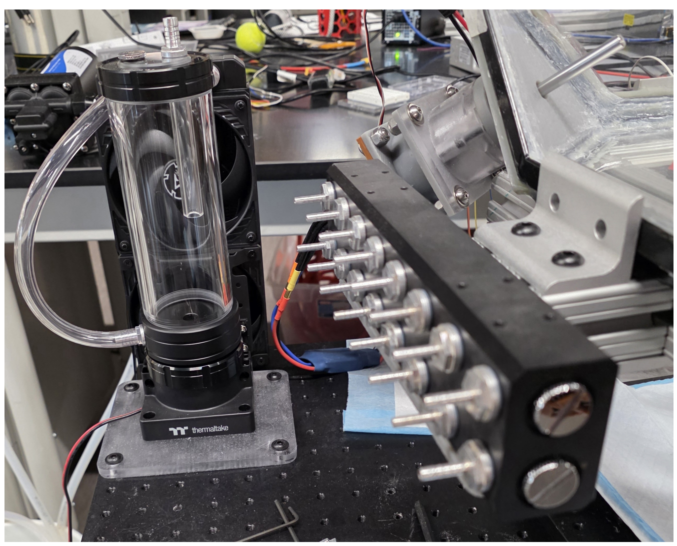

Figure 11: Water-cooling subsystem used for thermal management of the motor-drive system during integrated operation.

6.3 Preliminary System Tests

An important first stage of chamber validation is the performance of preliminary system tests. These tests are intended to establish that the redesigned chamber operates as a functional physical platform before more detailed turbulence characterization is pursued.

One category of preliminary testing concerns mechanical integrity. This includes confirming that the chamber body, structural supports, and shaft-interface assemblies remain physically stable during operation. Because the chamber contains multiple rotating components and is intended for liquid-phase experiments, practical issues such as alignment, structural support, sealing, and vibration are all relevant to this initial stage.

A second category concerns drive-system operation. Since the chamber depends on distributed impeller forcing, the ability of the eight motor assemblies to start, run, and remain in coordinated operation is a central systems-level requirement. A third category concerns control-system functionality, including encoder readout, RPM estimation, PWM distribution through the PCA9685, and PID-based motor-speed balancing.

A representative result from the preliminary control tests is shown in Figure 12. In this test, multiple motor-speed traces rise rapidly from startup and then converge toward a nearly common steady operating range. The close agreement among the RPM traces during the steady portion of the test indicates that the integrated control architecture can support synchronized multi-motor operation at an initial level.

The startup portion of the response shows that the motors do not reach the target state in exactly the same manner, which is expected in a practical multi-motor system with real hardware variation. However, after the transient phase, the measured speeds remain clustered within a relatively narrow band, suggesting that the encoder-based feedback and PWM-distribution architecture are functioning as intended. This is especially important because the chamber includes motors with different nominal KV ratings, making open-loop matching alone insufficient for reliable synchronization.

These preliminary system tests should therefore be interpreted as part of the validation contribution rather than as merely routine setup checks. They demonstrate that the chamber can be operated as an integrated, measurable, and repeatable electro-mechanical platform, even though full fluid-dynamic validation remains part of future work.

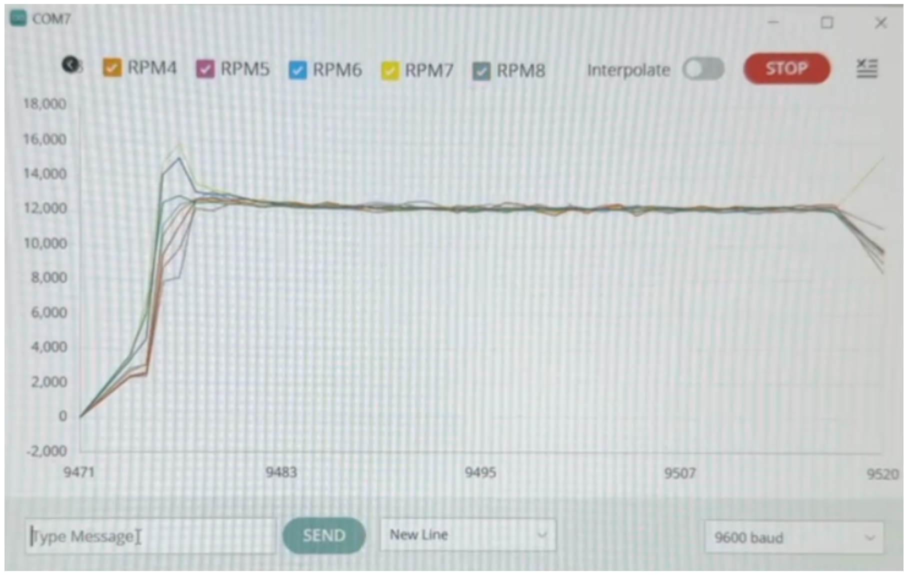

Figure 12: Representative RPM traces from preliminary integrated control testing of the redesigned chamber. The motor speeds approach a common steady operating range after startup, showing initial evidence of synchronized multi-motor operation.

6.4 Initial Flow Characterization

At the present stage, full flow characterization has not yet been completed. However, it is still useful to define the principal metrics by which the redesigned chamber will ultimately be evaluated. These include mean velocity, root-mean-square velocity fluctuations, isotropy ratios, probability density functions of velocity fluctuations, and turbulent energy spectra [1, 2]. Together, these quantities provide the basis for determining whether the chamber generates a flow that reasonably approximates homogeneous isotropic turbulence.

The earlier chamber study established an appropriate reference framework for such validation, and future measurements of the redesigned chamber should therefore be interpreted in continuity with that framework [4]. Comparable diagnostics are commonly used in laboratory HIT facilities based on jets, fans, and enclosed stirring systems [14, 11]. In this sense, the present work establishes the chamber and its control system, while also defining the path for later flow-field validation.

6.5 Comparison with the Previous System

A meaningful way to interpret the redesigned chamber is to compare it with the previous system that served as the baseline for this work [4]. Such a comparison can be made in terms of design scale, control architecture, sensing capability, and readiness for future experimentation.

From a mechanical standpoint, the redesigned chamber differs from the earlier device primarily in scale and in the associated need for revised structural and assembly features. The new chamber preserves the general impeller-driven concept of the earlier system, but adapts it to a larger physical platform with improved access features, revised sealing, and more complex corner drive units.

From a control standpoint, the difference is more direct. The previous chamber relied primarily on open-loop motor operation, whereas the redesigned chamber incorporates encoders, external PWM distribution, and PID-based speed balancing [4]. The new chamber should therefore be viewed not only as a larger structure, but also as a more instrumented and more controllable system.

From the perspective of validation, the earlier chamber provides the reference framework for what complete characterization would involve. The present work extends that framework by establishing a chamber that is better prepared for controlled operation and future diagnostics. A summary of the main differences between the previous chamber and the redesigned chamber is provided in Table 4.

Table 4: Comparison between the previous chamber and the redesigned chamber.

Category	Previous chamber	Redesigned chamber
Overall size	Smaller chamber geometry	Larger chamber geometry with approximately 20 in motor-to-motor spacing
Primary research emphasis	Focused more on microgravity-related applications	Focused more on turbulence generation and chamber development
Controller board	Arduino Mega	Arduino GIGA R1
Logic-voltage environment	5 V controller logic	3.3 V controller logic with level-shifting interface
Motor feedback	No encoder-based balancing	Encoder feedback added for all motors
Corner printed components	Corner mount, base mount, and motor housing	Corner mount, base mount, motor housing, and additional encoder piece
Control method	Primarily open-loop motor driving	PID-based feedback control added
PWM signal generation	Controller-based ESC signal generation	PCA9685-based PWM distribution with controller-side feedback processing
Power source	Battery-based power supply	Switching DC power supply
Bottom access design	Bottom cover without added circular access hole	Bottom panel modified to include a circular opening and removable cover
Top/bottom chamber access	More limited access configuration	Improved access through dedicated top and bottom openings
Cooling system	No dedicated motor-cooling subsystem	Water-cooling system added for motor thermal management
Sealing method	Epoxy sealing	Silicone plus epoxy sealing
System complexity	Lower integration complexity	Higher integration complexity with additional control, sensing, and support subsystems
Estimated cost	Relatively lower	Relatively higher
Validation emphasis	Earlier chamber served as prior experimental platform	Current chamber emphasizes redesign, construction, control integration, and preliminary system validation

6.6 Current Limitations

At the present stage of development, the redesigned chamber should still be understood as a platform in active refinement. Although the chamber has been designed, constructed, and integrated with improved control capability, this does not imply that every aspect of its final experimental characterization has already been completed.

The first limitation concerns the extent of flow validation. Full turbulence characterization requires detailed velocity-field measurements and statistical analysis, and such work remains part of the next stage of the project [4, 6]. The present thesis therefore distinguishes clearly between what has already been demonstrated—namely, construction, integrated operation, and initial control-level performance—and what still remains to be established through more extensive flow diagnostics.

A second limitation concerns controller refinement. Even with encoder integration and PID-based control in place, the final quality of synchronization still depends on implementation details such as gain selection, signal quality, and practical operating conditions. Some aspects of closed-loop performance may therefore require additional refinement before the chamber reaches its final operating state.

A third limitation is that improved motor-speed synchronization does not by itself prove final turbulence quality. Better synchronization is an important and well-motivated improvement, but it must ultimately be connected to flow-field measurements rather than inferred solely from control performance.

Despite these limitations, the redesigned chamber represents a significant advancement over the previous baseline in terms of scale, instrumentation, controllability, and system integration. The combination of mechanical construction, encoder integration, and initial system-level testing provides a strong basis for the broader interpretation and conclusions presented in the following chapters.

Chapter 7

Discussion

7.1 Interpretation of the Redesign

The redesigned chamber should be understood as an engineering advancement of the previous laboratory platform rather than as a completely separate device. Its main contribution lies in combining a larger chamber geometry with improved control, sensing, and supporting hardware. In this sense, the redesign is both mechanical and operational: the chamber body was enlarged, the corner drive assemblies were revised, encoder feedback was introduced, and the control architecture was upgraded from a simpler open-loop configuration to a more instrumented closed-loop system [4].

A central outcome of the redesign is that the chamber is now better suited to serve as an experimental platform. The earlier chamber established that the impeller-driven truncated-cube concept could generate approximately homogeneous isotropic turbulence. The present work extends that foundation by improving the controllability and practical operability of the system. This is important because future turbulence experiments depend not only on geometric design, but also on the ability to run the full motor array in a measurable and repeatable way. More broadly, the present chamber also fits within the continuing development of non-grid laboratory approaches for approximately homogeneous isotropic turbulence generation [10].

7.2 Mechanical and Experimental Significance

From a mechanical standpoint, the redesigned chamber is significant because it preserves the useful structural logic of the previous platform while adapting it to a larger and more complex system. The enlarged chamber body required revised corner interfaces, improved access covers, stronger attention to sealing, and a more developed support structure. These are not minor construction details; they are essential features that determine whether the chamber can function reliably as a liquid-phase experimental device.

The addition of improved top and bottom access also increases the experimental practicality of the system. A chamber intended for future turbulence and multiphase-flow studies must allow filling, draining, maintenance, and interior access without excessive disassembly. Similarly, the inclusion of water cooling reflects a practical design response to the thermal demands of prolonged multi-motor operation. These additions reinforce the idea that the chamber is not only a geometric object, but also a working laboratory platform.

7.3 Importance of Encoder-Based Control

One of the most meaningful differences between the redesigned chamber and the previous system is the introduction of encoder-based motor feedback. In the earlier configuration, motor operation depended more directly on open-loop driving. In the present chamber, encoder measurements make it possible to evaluate motor speed continuously and to apply feedback-based correction through PID control. This change directly addresses one of the practical limitations identified in the previous chamber study [4].

This improvement is especially important because the eight-motor array is not composed of identical motors. Since four motors are rated at 3250 KV and four are rated at 2660 KV, identical PWM commands do not imply identical operating speeds. Under these conditions, closed-loop speed balancing is not simply a convenience; it is a necessary part of preserving the approximate forcing symmetry required by an impeller-driven HIT chamber. PID-based regulation remains one of the most practical approaches for BLDC motor control [18]. More advanced synchronization strategies have also been proposed for multi-motor systems [19, 20].

The preliminary RPM results indicate that the upgraded control architecture can bring the motor speeds into a common operating range after startup. Although this does not by itself prove final turbulence quality, it is nevertheless a meaningful result. It shows that the redesigned chamber now has an instrumentation and control layer that was not present in the previous system and that this layer functions at the full eight-motor level.

7.4 Relation Between Control Performance and Turbulence Quality

An important point in interpreting the present work is that improved control performance and improved turbulence quality are related, but they are not identical. Better motor synchronization helps reduce forcing asymmetry and therefore supports the conditions needed for approximately homogeneous isotropic turbulence. However, turbulence quality must ultimately be assessed through flow-field measurements and statistical analysis rather than inferred from RPM agreement alone [1, 2].

For this reason, the present thesis should be read as establishing the chamber-level and control-level foundation for later turbulence validation. The redesign does not eliminate the need for PIV measurements, isotropy analysis, or spectral characterization. Instead, it creates a more suitable platform on which those measurements can be carried out in future work [6, 4]. This distinction is important because it defines the actual contribution of the thesis: the construction of a better-prepared chamber, not yet the completion of the full experimental turbulence campaign.

7.5 Relevance for Future Experiments

The redesigned chamber is relevant not only as a turbulence generator but also as enabling infrastructure for future experimental studies. From the standpoint of HIT research, its value lies in the possibility of combining a relatively accessible chamber design with improved controllability and more systematic operation. In this respect, the present chamber can be viewed alongside other enclosed or stirred laboratory platforms developed for approximately homogeneous isotropic turbulence generation [10, 14, 11].

Recent work has also demonstrated alternative enclosed and rapidly forced configurations for approximately homogeneous isotropic turbulence generation. These studies collectively show that practical laboratory HIT platforms continue to evolve in geometry, forcing method, and measurement capability.

From the standpoint of multiphase flow, the chamber is also valuable because approximately HIT provides a relatively clean environment for studying how turbulence interacts with dispersed phases [5]. This is one of the reasons why turbulence facilities of this general type are relevant to bubble and droplet studies [12, 13]. Once the redesigned chamber has been more fully characterized, it should provide a useful platform for future investigations of bubble motion, breakup, and turbulence–dispersed-phase interaction.

7.6 Overall Assessment of the Present Platform

Taken as a whole, the redesigned chamber represents a substantial improvement over the previous baseline in terms of size, instrumentation, controllability, and experimental readiness. The chamber is larger, better integrated, and more capable of supporting future controlled studies. At the same time, the redesign preserves the core concept that made the previous system valuable: a practical, in-house fabricated, impeller-driven chamber for experimental turbulence research [4].

The present platform therefore occupies an intermediate but important stage of development. It is more advanced than a simple construction prototype because it already integrates mechanical assembly, encoder feedback, PWM distribution, and preliminary synchronized operation. At the same time, it remains an experimental platform still awaiting full flow characterization. This dual status defines the central interpretation of the thesis: the work is successful as a chamber redesign and system-integration effort, and it establishes a clear basis for the next stage of turbulence and multiphase-flow experiments.

Chapter 8

Conclusions and Future Work

8.1 Conclusions

This thesis presented the design, construction, and initial validation of an enhanced homogeneous isotropic turbulence chamber developed as an enlarged and improved version of a previous laboratory platform. The work focused on platform development rather than on a complete turbulence-characterization campaign. Within that scope, the main objectives of the project were achieved.

From a mechanical perspective, the redesigned chamber was successfully enlarged and reconstructed as a more capable experimental system. The new design preserves the impeller-driven truncated-cube concept of the earlier chamber while incorporating revised corner drive assemblies, improved access openings, updated sealing methods, and a support structure suitable for a larger device. The resulting chamber is therefore not simply a scaled copy of the earlier system, but a more developed electro-mechanical platform [4].

From a control perspective, the chamber was upgraded from a simpler open-loop configuration to a more instrumented feedback-based system. The redesigned platform integrates eight encoders, an Arduino GIGA controller, a PCA9685 PWM-distribution module, level-shifting hardware, centralized power distribution, and PID-based motor-speed balancing. These additions directly address one of the important limitations of the previous system, namely the need for improved motor-speed synchronization across the impeller array [4].

From a validation perspective, the present work established that the redesigned chamber can operate as an integrated experimental platform. Preliminary system tests showed that the control architecture can support coordinated multi-motor operation and that encoder-based feedback can bring the motor speeds into a common operating range after startup. Although full flow characterization remains to be completed, the chamber has already advanced beyond the level of a purely structural prototype.

Taken together, these results support the main conclusion of the thesis: the redesigned chamber constitutes a meaningful improvement over the previous baseline in terms of size, instrumentation, controllability, and experimental readiness. The principal contribution of the work is therefore the successful development of a better-prepared platform for future turbulence and multiphase-flow experiments.

8.2 Future Work

The most important next step is full flow characterization of the redesigned chamber. This should include velocity-field measurements in the central region of the chamber and statistical analysis of the resulting data. In particular, future work should evaluate mean velocity, root-mean-square velocity fluctuations, isotropy ratios, probability density functions of the fluctuations, and turbulent energy spectra [1, 2]. These measurements are necessary to determine the extent to which the redesigned chamber reproduces the desired characteristics of approximately homogeneous isotropic turbulence [6, 4].

A second direction for future work is continued refinement of the control system. Although the present implementation already provides encoder-based balancing, additional improvements may still be possible through further tuning of the PID gains, refinement of the update logic, and evaluation of synchronization performance under different operating conditions. Such work would strengthen the connection between control-level performance and final flow quality [20].

A third direction is the use of the redesigned chamber as a platform for future multiphase-flow studies. One of the motivations for improving chamber scale, access, and controllability is to support experiments involving dispersed phases such as bubbles. Once the redesigned chamber has been fully characterized in single-phase operation, it can serve as a better-controlled environment for studies of bubble motion, breakup, and turbulence–dispersed-phase interaction [5, 13].

Future work may also include practical hardware refinements. These could involve further optimization of wiring organization, thermal management, serviceability, and long-duration operating stability. While such refinements are secondary to the main chamber concept, they can still improve the repeatability and usability of the platform in later experiments.

In summary, the present thesis completes an important platform-development stage but not the final experimental program. Its main value lies in establishing the enlarged chamber and its integrated control architecture as a workable foundation for the next stage of turbulence validation and multiphase-flow research.

Bibliography

[1] S. B. Pope, *Turbulent Flows.* Cambridge University Press, 2000.

[2] H. Tennekes and J. L. Lumley, *A First Course in Turbulence.* MIT Press, 1972.

[3] E. A. Variano and E. A. Cowen, “A random-jet-stirred turbulence tank,” *Journal of Fluid Mechanics*, vol. 604, pp. 1–32, 2008.

[4] M. E. Federle, B. Lyons, M. Ravisankar, and R. Zenit, “Design of an accessible turbulence chamber for laboratory experiments,” *HardwareX*, vol. 25, p. e00745, 2026.

[5] F. Risso and J. Fabre, “Oscillations and breakup of a bubble immersed in a turbulent field,” *Journal of Fluid Mechanics*, vol. 372, pp. 323–355, 1998.

[6] M. Raffel, C. E. Willert, F. Scarano, C. J. Kähler, S. T. Wereley, and J. Kompenhans, *Particle Image Velocimetry: A Practical Guide*, 3rd ed. Springer, 2018.

[7] E. Rathakrishnan, *Instrumentation, Measurements, and Experiments in Fluids*, 2nd ed. CRC Press, 2017.

[8] C. Tropea, A. L. Yarin, and J. F. Foss, Eds., *Springer Handbook of Experimental Fluid Mechanics.* Springer, 2007.

[9] R. Zimmermann, H. Xu, Y. Gasteuil, M. Bourgoin, R. Volk, J.-F. Pinton, and E. Bodenschatz, “The Lagrangian exploration module: An apparatus for the study of statistically homogeneous and isotropic turbulence,” *Review of Scientific Instruments*, vol. 81, no. 5, p. 055112, 2010.

[10] P. C. López-López and J. P. Solano, “Laboratory generation of zero-mean-flow homogeneous isotropic turbulence: non-grid approaches,” *Flow*, vol. 4, p. E1, 2024.

[11] M. Manna, M. S. Mansour, S. H. Chung, and W. L. Roberts, “Characterization of turbulence in an optically accessible fan-stirred spherical combustion chamber,” *Combustion Science and Technology*, vol. 193, no. 7, pp. 1231–1257, 2021.

[12] L. Beckedorff *et al.*, “Jet-stirred homogeneous isotropic turbulent water tank for bubble and droplet fragmentation,” *Review of Scientific Instruments*, vol. 96, no. 2, p. 025107, 2025.

[13] S. Li, D. R. González, and S. Menon, "V-ONSET (vertical octagonal noncorrosive stirred energetic turbulence): A vertical water tunnel with a large energy dissipation rate to study bubble/droplet deformation and breakup in strong turbulence," *Review of Scientific Instruments*, vol. 95, no. 1, p. 015101, 2024.

[14] Z. Dou, Z. K. Pecenak, L. Cao, S. H. Woodward, Z. Liang, and H. Meng, "PIV measurement of high-Reynolds-number homogeneous and isotropic turbulence in an enclosed flow apparatus with fan agitation," *Measurement Science and Technology*, vol. 27, no. 3, p. 035305, 2016.

[15] R. X. Perez, *Mechanical Seals and Flush Plans.* Wiley, 2022.

[16] L. A. Horve, *Shaft Seals for Dynamic Applications.* CRC Press, 1996.

[17] J. Fraden, *Handbook of Modern Sensors: Physics, Designs, and Applications*, 5th ed. Springer, 2016.

[18] A. Arora, S. Gawade, and N. Zope, "Simulation of synchronization control strategies and energy consumption in multi-motor systems for electric vehicles," *Engineering Research Express*, vol. 7, p. 035309, 2025.

[19] J. Li, X. Wang, and Y. Zhang, "Synchronous control of multiple motors based on deviation coupling," in *Proceedings of the 2024 IEEE International Conference on Industrial Technology (ICIT)*, 2024, pp. 1–6.

[20] Y. Mu, L. Qi, M. Sun, and W. Han, "An improved deviation coupling control method for speed synchronization of multi-motor systems," *Applied Sciences*, vol. 14, no. 12, p. 5300, 2024.